Utilizing Qs and Qk to Model TE Materials for Predicting Temperature Dependence

Richard J. Buist
TE Technology, Inc., 1590 Keane Drive, Traverse City, MI 49686 USA
Phone: (616) 929-3966, FAX: (616) 929-4163, E-mail: <cool@tetech.com>

Abstract

The parameters, Qs and Qk, were first introduced by Tuomi [1],[2] in the early 1960's from research contracted to The Franklin Institute. The purpose of this research was to create a method for characterization of thermoelectric (TE) materials which was independent of the dopant level This would quickly and easily determine the potential of a TE material from a single experiment. This was applied by Tuomi, thereby eliminating the need for many separate experiments needed to optimize the dopant level to establish what the maximim Figure of Merit (Z) could be. These parameters, Qs and Qk were based on solid-state physics single-band theory, electron and phonon scattering laws and empirically derived activation energies for electrons and holes in semiconducting materials used in thermoelectric cooling applications. They were named Qs = Quality with respect to Seebeck [3] and Qk = Quality with respect to Kappa (thermal conductivity) [4]. Originally, The Borg-Warner Research Center had a moratorium against releasing research information to the general public which included work on TE materials. Now, these findings and a more thorough analysis have been recently published by Tuomi [5] at ICT97, Dresden, Germany.

One of the principles of the Qs/Qk theory is that these quantities are invariant to changes in carrier concentration. The author recognized that (at least over a limited temperature range) the transport parameter variance may be quite the same whether carriers are created by thermal excitation or via doping changes. This lead to the hypothesis that, using these Qs/Qk curves, the temperature dependence of the TE material kinetic properties can be determined from a single test point of the Seebeck Coefficient, α, Thermal conductivity, κ, and electrical conductivity, σ at some known temperature.

Temperature dependent test data is presented and plotted against the Qs/Qk curves and the theoretically generated temperature dependent curves for each TE material parameter. Test data from TE material doping experiments is also presented to validate the correlation with that predicted from the Qs/Qk theory.

The limitations are also demonstrated by presentation of test data at temperature extremes where ambipolar conduction effects emerge and the assumption of single band theory breaks down.

Introduction

The quantity "Qs" roughly corresponds to the product of carrier effective mass x mobility product. The quantity "Qk" corresponds to the projected thermal conductivity at zero carrier concentration, analogous to the lattice thermal conductivity. Since Qs and Qk are relatively invariant with carrier concentration, these parameters have been effectively used by Tuomi for evaluating many different kinds and classes of materials for their thermoelectric potential.

The author has also used these parameters extensively, but for another purpose. These parameters, plus specimen test data from a single test point, were used to forecast the TE parameter temperature dependence, thereby proving the key information needed to design and optimize TE devices whenever only a single test point is available.

Test Method

The test method employed to test small, pellet-shaped specimens was the temperature-dependent test system, model TF-101 manufactured by TE Technology, Inc., pictured in Figure 1. This unique test process was described by Buist [6],[7].

Each specimen was soldered between two nickel plated cooper tabs and wired with very small type-T thermocouples and current leads on each tab. Individually and separately, they were then physically and thermally attached to the top of a TE cascade (see insert in Figure 1) used to create a wide range of temperatures. All tests were performed in a vacuum of less than 0.02 milliTorr. Specimen geometry was optimized to yield minimum errors due to radiation conduction allong the test leads. The calculated maximum error due to these effects was typically less than 1%.

TE Material Specimen

TE materials specimens were obtained from many of the leading manufacturers of TE materials from all over the world. Sources included some organizations from Russia, Ukraine, Japan and several from the USA. The dimensions were 2 to 5 mm square by 1.5 to 2mm long.

Over 100 specimens were collected and tested but not all were used in this analysis because of their similarity with other samples. Nevertheless, data from 24 P-type specimens and 28 N-type specimens were presented and analyzed herein.

Temperature Dependent Test Data

Test data was obtained from 24 P-type and 28 N-type specimens. The TE materials of interest were those which are typically used in TE cooling applications. They were chosen to provide the widest spread in properties possible, with minimum duplication.

Figures 2 and 3 illustrate the Z versus temperature for all specimens tested. It is clear that the variance in properties and temperature dependence was dramatically different for

both N-type and P-type specimens. These curves also illustrate how errant it would be to simply scale TE properties to some "standard" using a single test point.

Analytical Technique

In spite of this obvious variance, it was discovered that the logarithm of σ, versus the logarithm of temperature for each specimen produced essentially linear curves, as shown in Figures 4 and 5. The major significance, however, was that, they were all quite parallel when P-type and N-type were considered separately! This was the key to calculating the temperature dependence of each TE parameter, σ, κ, and α.

In order to minimize the "clutter". A selected, smaller set of specimens were chosen to cover the range of properties obtained. The selection process was to determine the "outlier" Z values for sequential steps of σ. Eight (8) sets each of N-type and P-type specimen test data were used for the subsequent temperature dependent forecast calculations.

Temperature Dependent Forecast for σ

The first step in this process was to define σ vs. Temperature, using the common slope from either Figure 4 (N-type) or 5 (P-type), whichever applied. Essentially, the tested, room temperature value of σ was recalculated in order to plot this point on Figure 4 or 5. The all-important temperature dependence of σ was calculated by drawing a line parallel to its neighboring lines on the graph. The resulting calculations (shown as curves) were plotted against the tested σ values for each specimen (shown as symbols) in Figures 6 and 7. It is observed that the agreement between calculated and actual test data is quite good, as was implied by the parallelism of the linear curves in Figures 4 and 5.

The calculated σ vs. Temperature for both N and P-type TE materials is a very important link to temperature dependent forecast calculations. That is, to determine the forecasted values of κ, α, Z vs. Temperature, one only needs to relate κ with σ variance and α with σ variance in order to determine κ vs. Temperature and α vs. Temperature. Finally, with all three TE properties determined, the formula, $Z = \alpha^2\sigma/\kappa$, yields the forecasted Z temperature dependence.

The relationship between σ and κ (via varying dopant concentration) is specified by the parameter, Qk, as discussed above. Similarly, the relationship between σ and α (via varying dopant concentration) is the parameter, Qs, also discussed above. That is, Qk and Qs are essentially constant with respect to carrier concentration. The hypothesis of this analysis was that, over some specified temperature range, it does not matter whether carrier concentration is changed by dopant level or temperature-variant-produced carrier concentration. This specified range is where the TE material is extrinsic, i.e. where carriers are created by ionization of impurities. Under these conditions, both Qk and Qs were expected to be nearly constant with respect to temperature. Thus, κ vs. temperature can be calculated from the room temperature tested, "constant" Qk and the established σ vs. temperature established above. Similarly, α vs. temperature , can be calculated from the room temperature tested, "constant" Qs and the established σ vs. temperature established above.

Temperature Dependent Forecast for κ

The first step in this process was to plot κ versus σ from the entire data base of tested parameters versus temperature to test the assumption of constant Qk versus temperature for a wide variety of TE materials. This data is shown in Figures 8 (N-type) and 9 (P-type). If one were to delete all of the data points except the room temperature points, the variance in this abbreviated set of data will clearly indicate the linear patterns consistent with the plotted lines shown in Figures 8 and 9. This clearly substantiates the validity of the dopant-driven, constant Qk for a given primary composition.

The data to the right is characterized by larger doping levels and/or colder temperatures. This would be the expected operable range of the subject forecast calculation process, since the TE materials are more extrinsic in this region. That is, ambipolar, electron/hole pair production is quite non-existent in this region.

The data to the left is characterized by smaller doping levels and/or hotter temperatures. This intrinsic mode results in ambipolar, electron/hole pair production. This produces more and more carriers as we move to the left (hotter temperatures) which increases κ (affected by both carrier types) However, σ decreases because it does not benefit from the electron/hole pair production which essentially cancel themselves out. In fact, the increasing κ to the left is a classic representation of intrinsic behavior.

Nevertheless, the test data from the representative smaller set of test data (8 specimens each of N and P-type) was used to calculate κ from the room temperature, tested Qk and the set of σ data calculations (curves) shown in Figures 6 and 7. The resulting temperature dependence is shown in Figures 10 and 11. Again, the resulting κ calculations (shown as curves) were plotted against the tested κ values for each specimen (shown as symbols) in these charts. It is clear that these curve-fits to the actual test data are not as good as those for σ vs. temperature. This is a result of the obvious ambipolar phenomenon evidenced in the left portion of Figures 8 and 9. In fact Figure 9 (P-type) exhibited less ambipolar conduction resulting in better P-type κ calculations versus temperature than for N-type.

Temperature Dependent Forecast for α

This process was very similar to that for calculating the temperature dependence of κ from the room temperature test point. The only generic difference was that Qs and α were used with the derived σ temperature dependence instead of Qk and κ. Again, the entire data base of tested α vs. σ parameters were plotted versus temperature to test the assumption of constant Qs versus temperature for a wide variety of TE materials. This data is shown in Figures 12 (N-type) and 13 (P-type). Similar to the Qk graphs, deleting all of the data points except the room temperature points will

clearly indicate the patterns consistent with the plotted constant Qs curves shown in Figures 12 and 13. Again, this clearly substantiates the validity of the dopant-driven, constant Qs for a given primary composition.

The ambipolar, electron/hole pair production is quite prevalent to the left side of the chart where intrinsic conduction occurs at the hotter temperatures and lower doped materials. The data to the right is characterized by larger doping levels and/or colder temperatures. where more extrinsic conduction is evidenced. That is, as was for the Qk curves, the ambipolar, electron/hole pair production is quite non-existent in this region where better curve-fits are to be expected.

The data to the left exhibits a drop-off in α due to the lowering of the mobility of majority carriers due to the ever-increasing concentration of total carriers without much change in the net majority carrier concentration. In essence, the TE material lattice is becoming very crowded with the onset on electron/hole production. This makes it more difficult for the ever-decreasing net concentration of majority carriers to easily proceed through the lattice.

It is interesting to note that these two curves plotted together with the negative sign used for N-type, the famous "Price Loop" appears (at least in form) but due to temperature dependence rather than via dopant concentration. Again, this gives further credence to the basic equivalency of producing carriers by thermal means and increasing dopant concentration.

The test data from the same representative smaller set of test data (8 specimens each of N and P-type) was used to calculate α from the room temperature, tested Qs and the set of σ data calculations (curves) shown in Figures 6 and 7. The resulting temperature dependence is shown in Figures 14 and 15. Again, the resulting α calculations (shown as curves) were plotted against the tested α values for each specimen (shown as symbols) in these charts. These curve-fits to the actual test data are good in some cases (where extrinsic conduction prevails) but poor for others, mostly affected by intrinsic conduction. Nevertheless, the calculations still fit well with the tested data for several medium α TE material specimens. The problem, however, is that the disparity between calculations and test data for Z is expected to be even poorer since α is squared and divided by κ.

Temperature Dependent Forecast for Z

This was a rather simple process using the calculated σ, κ and α values in the formula for $Z = \alpha^2\sigma/\kappa$ to generate the predicted Z vs. temperature calculations. These data are plotted against the tested Z values as shown in Figures 16 and 17.

Note that some of the complicated curve crossing is still captured in these charts and that some cases, especially for N-type, fit fairly well for the mid-range cases especially considering the errors in σ are multiplied by the errors in κ multiplied by twice the errors in α calculations.

Conclusions

Considering the complicated temperature dependence of Z vs. temperature shown in Figures 2 and 3, it was a lot to expect to be able to accurately recreate these curves using only the test data from a single temperature test point. Nevertheless, results on some specimens fared quite well. These were for the cases where ambipolar conduction was less prevalent. This substantiates the hypothesis that the same curves generated by carriers produced by dopant concentration will apply to the case where carriers are produced by impurity ionization via thermal excitation.

The process presented in this paper is a good first start. The quality of next task is to expand the Qs and Qk curves to a 2-band model. This will capture and account for the ambipolar effects evident in the test data presented herein. The challenge of this expansion of the theory will be to establish the effective band gap and how it may be affected by temperature. If that can be done, the calculated projections will certainly be improved. This would yield a powerful tool for establishing acceptably accurate TE device models using only a single test data point to characterize the TE materials.

Finally, this process should be applicable to the high temperature materials used for power generation. Certainly the temperatures are higher, but if the band gaps are proportionally even higher, ambipolar effects will be suppressed and single-band theory will prevail. If so, the process described herein will accurately apply.

References:

[1] D. Tuomi, "Thermoelectric Material Quality – The Seebeck—Electrical Conductivity Relationship, Internal Report B-W-R #3259-01, (1962).

[2] D. Tuomi, "Notes on the Origins of Qs and Qk Characterizations of semiconductor Alloys", Internal Report, Borg-Warner Research Center, (1964).

[3] D. Tuomi, "Thermoelectricity: VII The Seebeck Quality Factor, Qs, a Semiconductor Characterization Tool", J. Electrochemical Soc. 131 (9) 2101, (1983).

[4] D. Tuomi, "Thermoelectricity: VIII The Thermal Conductivity Quality Factor, Qk, a Semiconductor Characterization Tool", J. Electrochemical Soc. 131 (10) 2319, (1983).

[5] D. Tuomi, " Structural Chemical Characterization of Semiconductors Using the Seebeck and Thermal Conductivity Quality Factors Qs and Qk", in Proceedings of the XVI Conference on Thermoelectrics, Dresden, Germany, (1997).

[6] R.J. Buist, "A New Method for Testing Thermoelectric Materials and Devices", 11th International Conference on Thermoelectrics, Arlington, TX, USA (1992).

[7] R.J. Buist, "Methodology for Testing Thermoelectric Materials and Devices", CRC Handbook of Thermoelectrics, CRC Press, Inc., (1995).

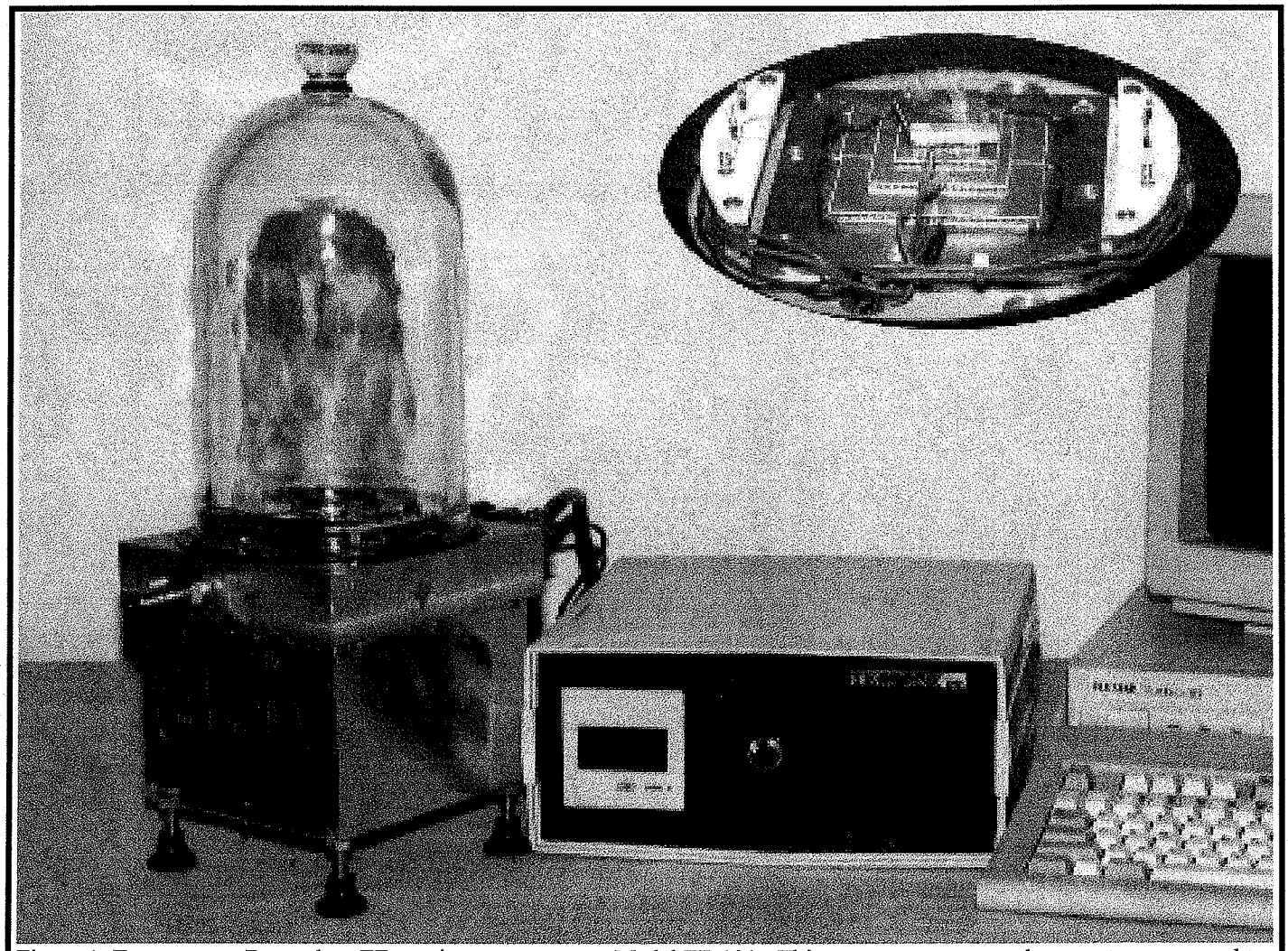

Figure 1. Temperature Dependent TE specimen test system, Model TF-101. This computer-automated test system was used to obtain all test data presented in this paper. Note the interior of the vacuum bell jar shown in the insert. A TE cascade is used to automatically cool and heat the TE material specimen to pre-selected temperatures from -60°C to +60°C. It employs the "Transient" method of testing, similar to the "Harman" method but modified to improve accuracy and repeatability. This was accomplished by utilizing the same DC measuring system and avoiding chopped, AC current. Furthermore, testing of Seebeck Coefficient, Resistivity, Thermal Conductivity and Z is made at the same, exact instant in time via an absolute method

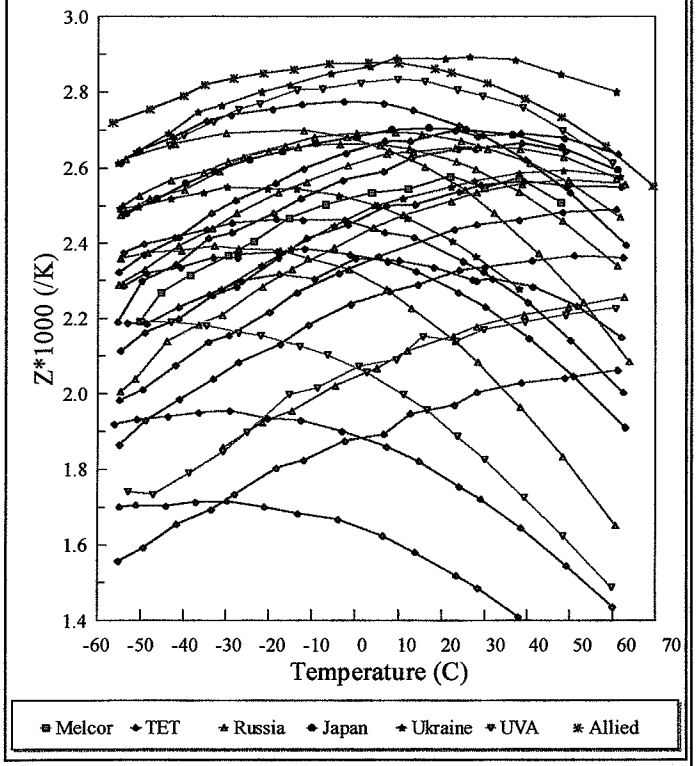

Figure 2. Tested Z for 28 selected N-type TE material specimens.

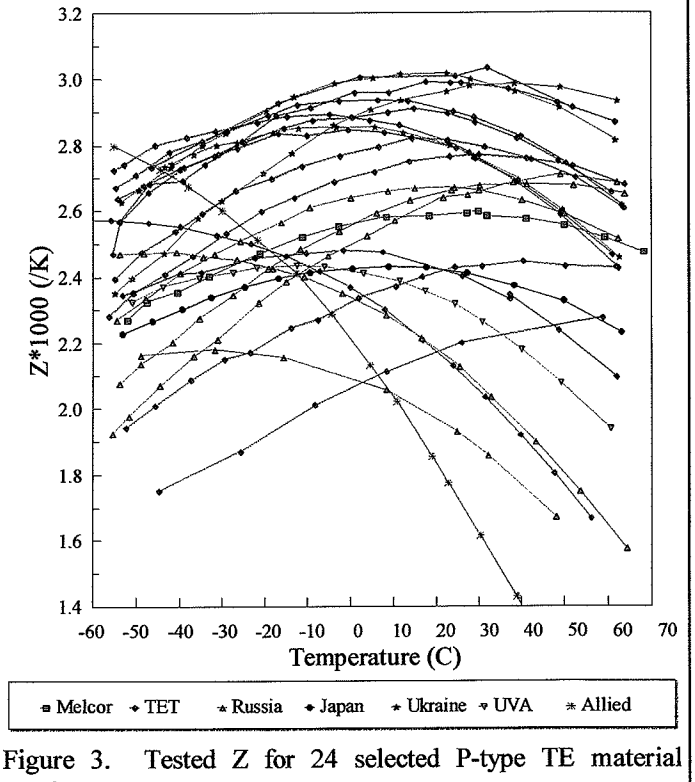

Figure 3. Tested Z for 24 selected P-type TE material specimens.

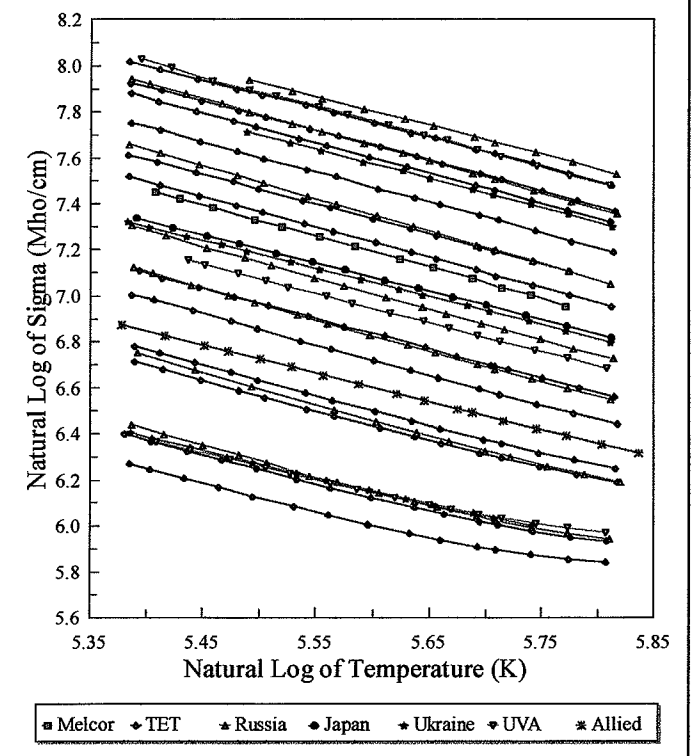

Figure 4. Linear dependence of logarithms of sigma versus temperature (K) for N-type TE material specimens.

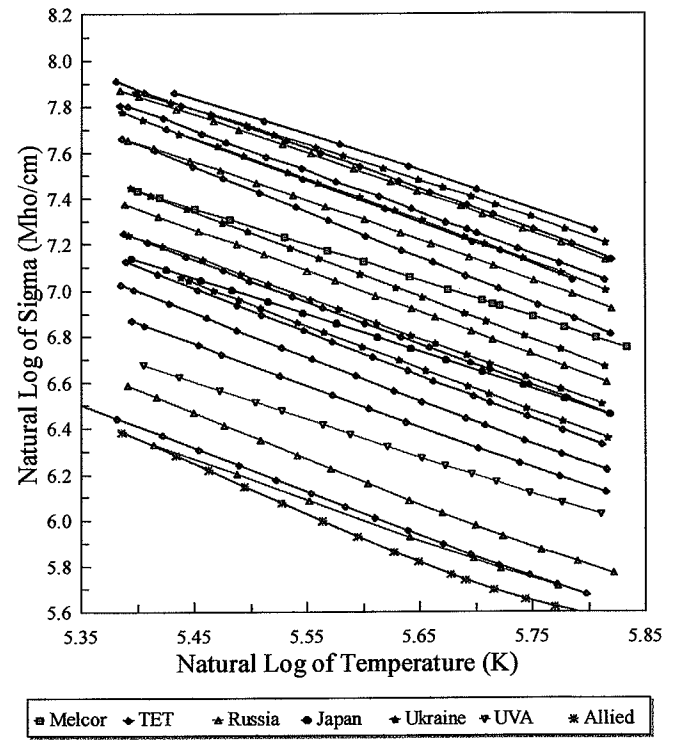

Figure 5 Linear dependence of logarithms of sigma versus temperature (K) for P-type TE material specimens.

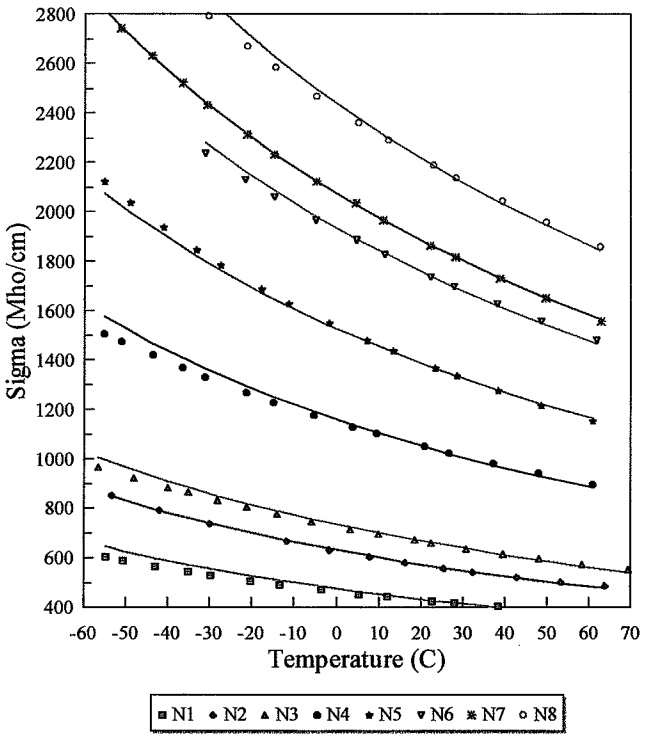

Figure 6. σ versus temperature for 8 N-type TE material specimens. Symbols = test data, Curves = Calculations.

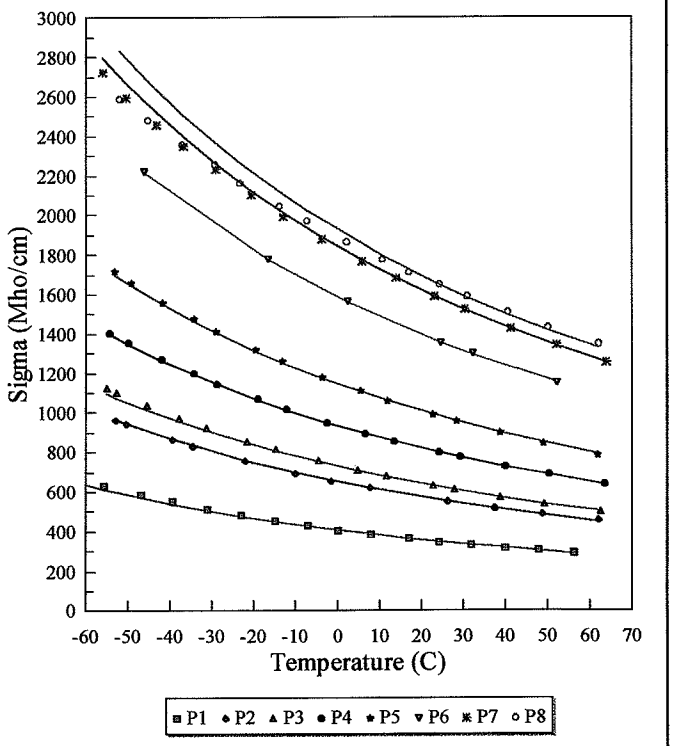

Figure 7. σ versus temperature for 8 P-type TE material specimens. Symbols = test data, Curves = Calculations.

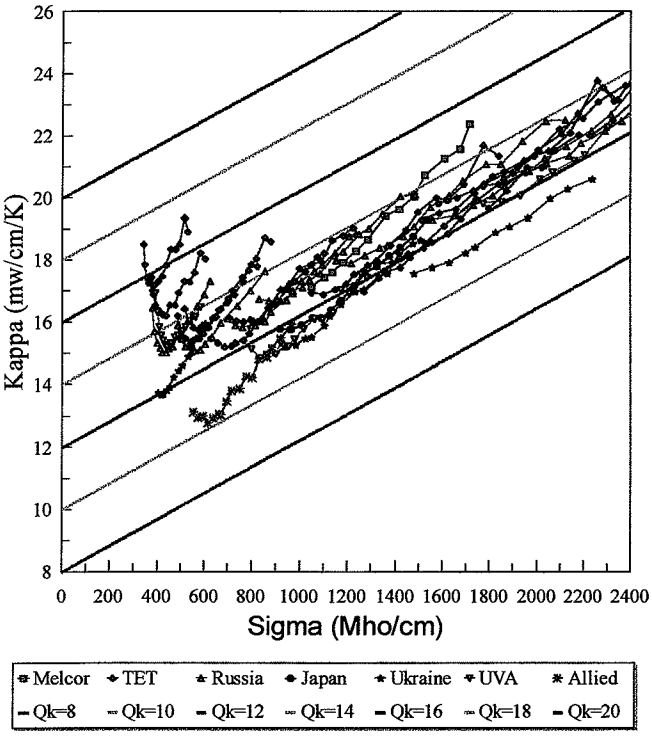

Figure 8. κ versus σ for 28 N-type TE material specimens. Symbols = test data, Curves = Calculations.

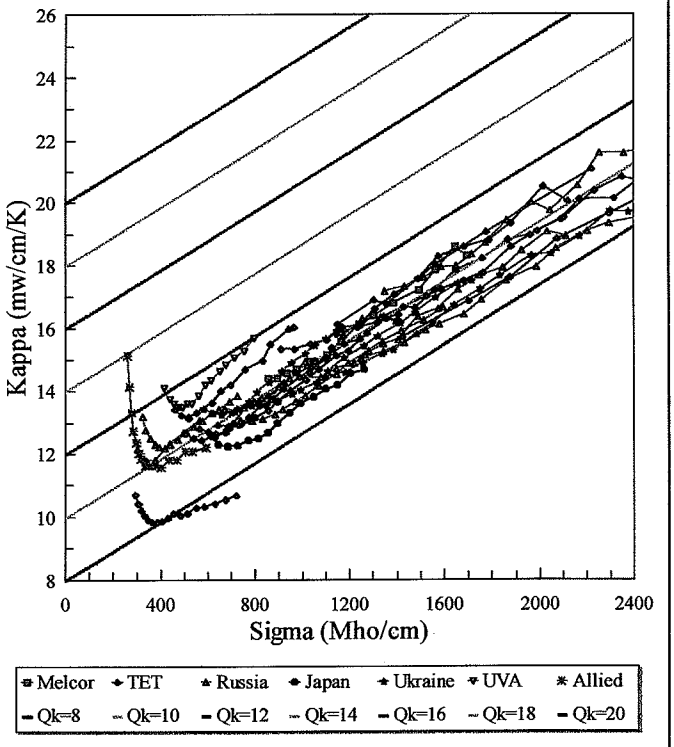

Figure 9. κ versus σ for 24 P-type TE material specimens. Symbols = test data, Curves = Calculations.

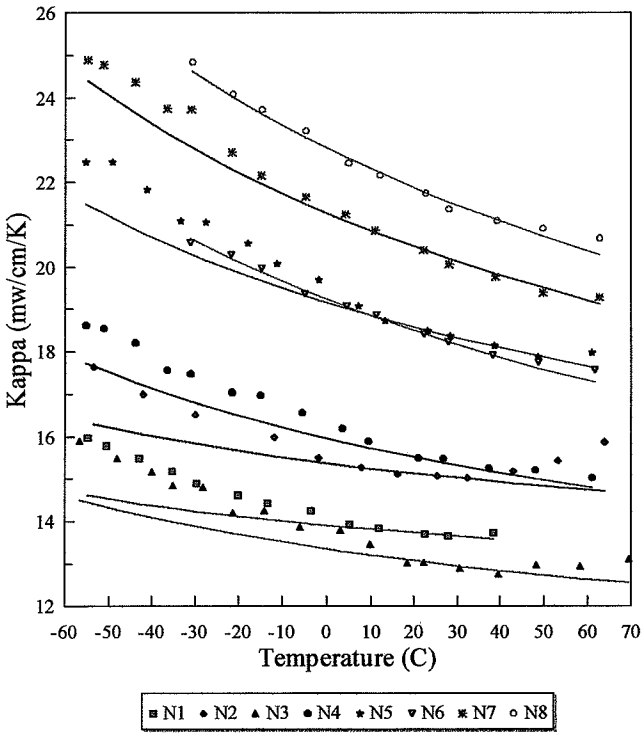

Figure 10. κ versus temperature for 8 N-type TE material specimens. Symbols = test data, Curves = Calculations.

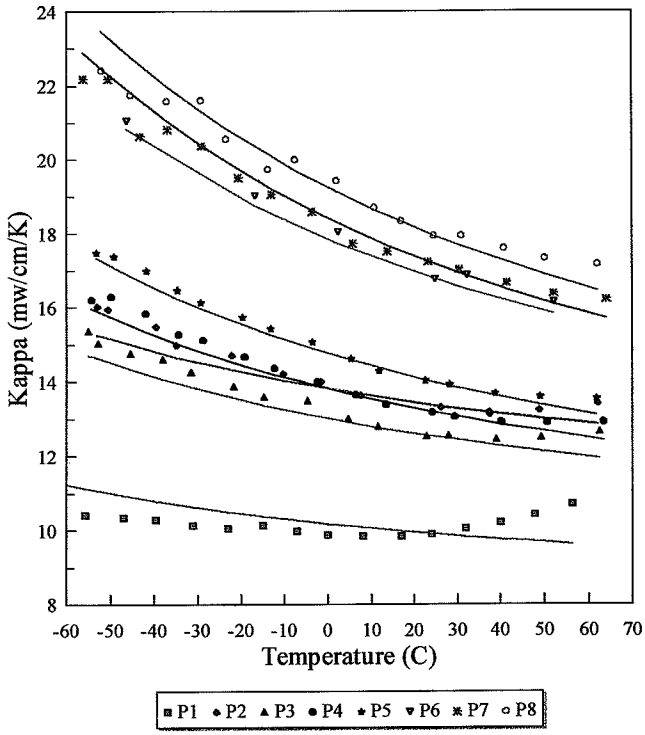

Figure 11. κ versus temperature for 8 P-type TE material specimens. Symbols = test data, Curves = Calculations.

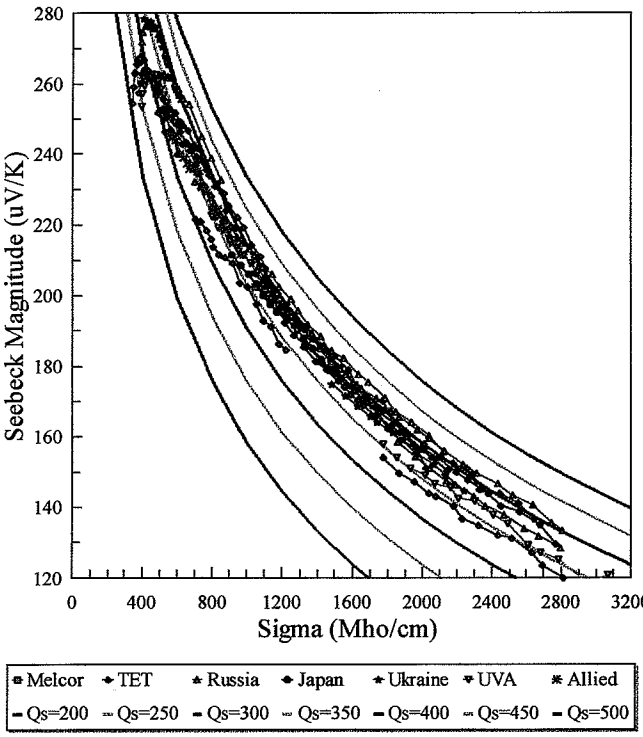

Figure 12. α versus σ for 28 N-type TE material specimens. Symbols = test data, Curves = Calculations.

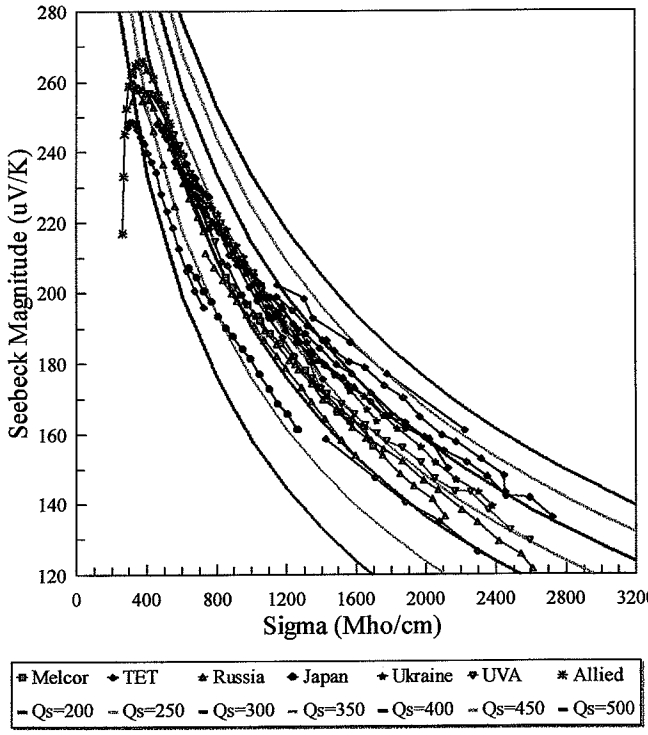

Figure 13 α versus σ for 24 P-type TE material specimens. Symbols = test data, Curves = Calculations.

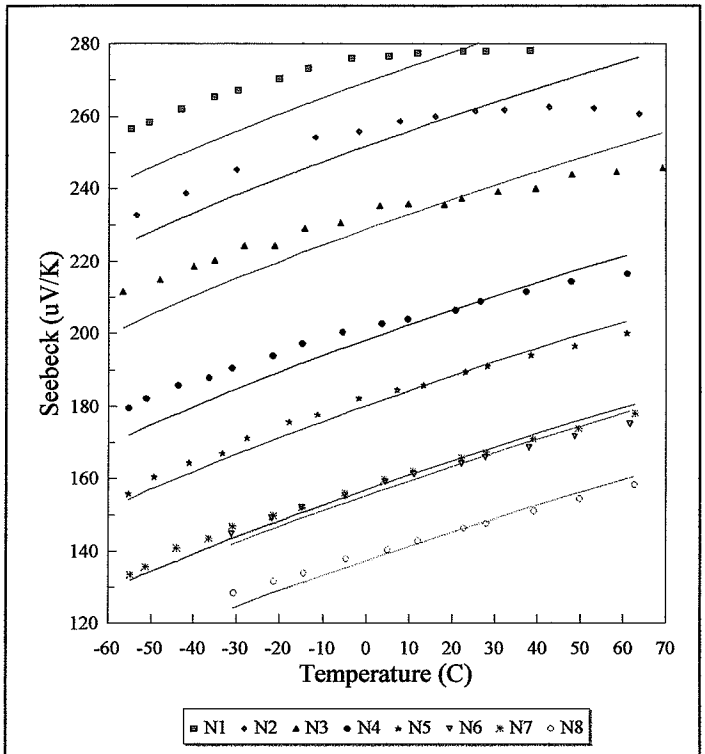

Figure 14. α versus temperature for 8 N-type TE material specimens. Symbols = test data, Curves = Calculations.

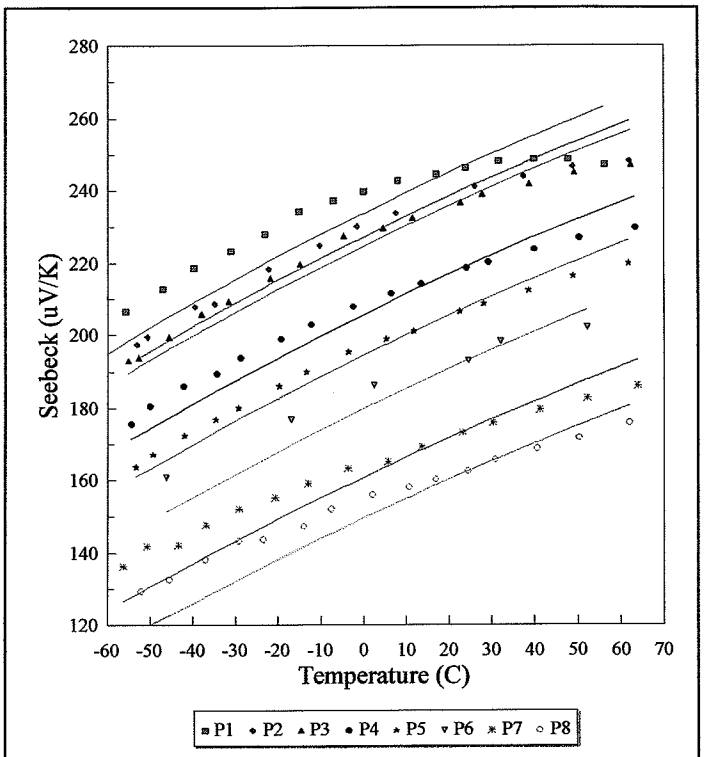

Figure 15. α versus temperature for 8 P-type TE material specimens. Symbols = test data, Curves = Calculations.

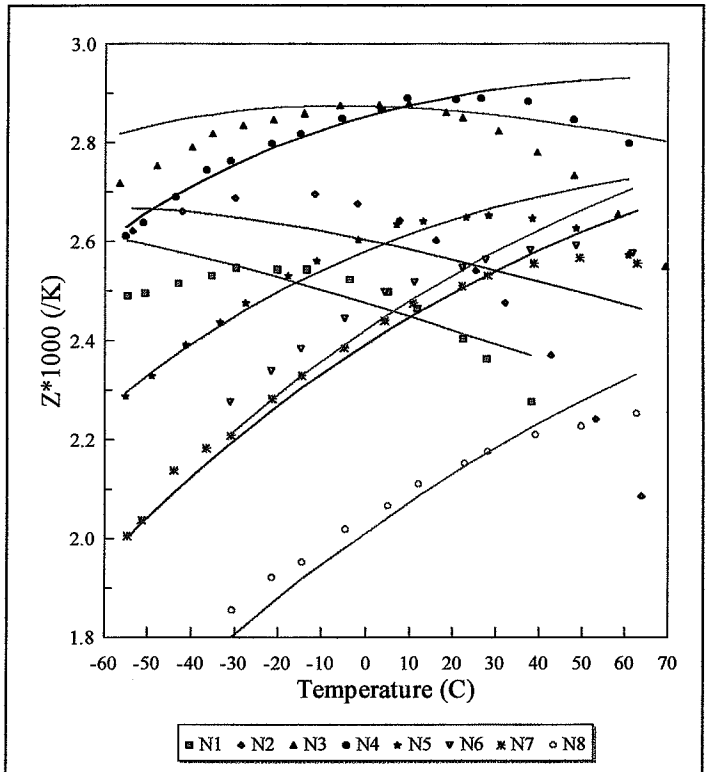

Figure 16. Z versus temperature for 8 N-type TE material specimens. Symbols = test data, Curves = Calculations.

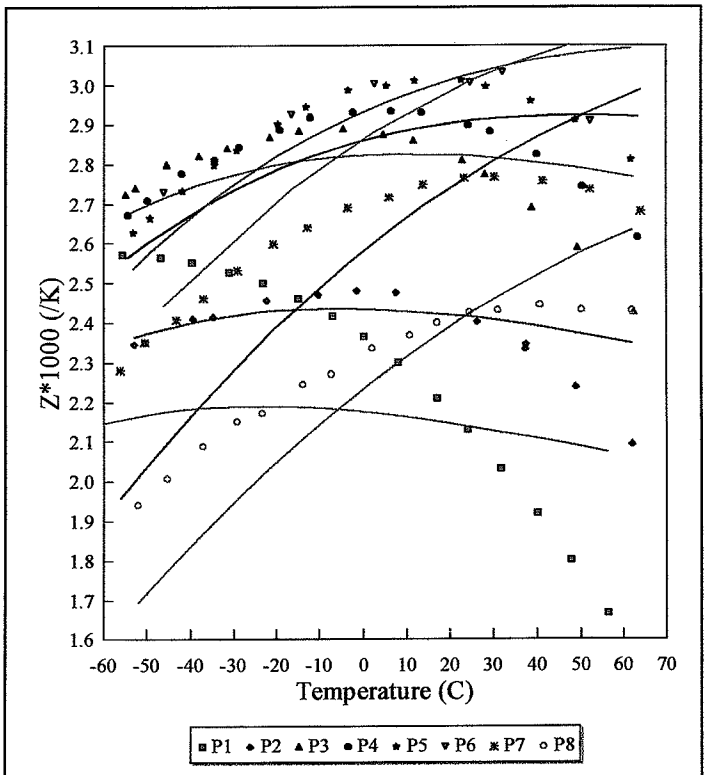

Figure 17. Z versus temperature for 8 P-type TE material specimens. Symbols = test data, Curves = Calculations.